Influence of core diameter on the 3-dB bandwidth of graded-index optical fibers

Comprehensive Theory of Dispersion in Graded-Index Optical Fibers

G. Yabre, *Member, IEEE*

***Abstract*—This paper presents a theoretical investigation on the dispersion in graded-index silica glass fibers under overfilled launching with equal excitation of modes. This theory incorporates both chromatic effect and modal contribution which takes not only the modal delay into account but also the distributed loss and mode-coupling. Random microbends are considered to be the most dominant source of coupling. All index perturbations and intrinsic core diameter variations are assumed to be negligible, but they could readily be included without changing the basic structure of the model. The 3-dB bandwidth is analyzed through the study of the fiber transfer function which introduces the wavelength and modal effects as two separate filter functions. The formal derivation of the chromatic transfer function is analytical. On the other hand, the modal transfer function is obtained by numerically solving the power flow equation in the frequency domain using Crank–Nicholson method. As an application, the results are illustrated showing, in particular, the influence of the fiber core/outside diameters, for the first time.**

***Index Terms*—Bandwidth, Crank–Nicholson method, differential modal attenuation, dispersion, graded-index optical fibers, mode-coupling, optical communications, power flow equation.**

I. Introduction

THE GROWING demand in data transmission, raised in particular by the Internet, will require the use of optical fibers as transmission media instead of coaxial cables, even at short distance. Coaxial cables are extremely lossy, susceptible to electromagnetic interference (EMI), and show a dramatic limitation in their capacity for digital transmission. On the other hand, optical fibers show a very low attenuation, a great potential for high-speed transmission and a complete immunity to EMI. This is true for single-mode fibers but also for the multimode versions, so either type of fibers can be employed in replacement of the metallic cables. However, more attention is being given to multimode fibers (MMF's) rather than single-mode fibers for use in local area networks (LAN's). Multimode fibers are easier to make and their large dimensions impose less stringent requirements on cabling, connecting, splicing and handling compared to the single mode version. Moreover, the large core region of multimode fibers added to their large numerical aperture allows for efficient light coupling from semiconductor lasers, which offers large mechanical tolerances in transceiver development. It is clear that in the short-range applications where many junctions and connections between adjacent sections are often necessary, the multimode version is the most appropriate in consideration of whole system cost.

Despite the above advantages, the use of multimode fibers has been resisted for some years by fiber-optic link designers in favor of single-mode fibers (SMF's) since Epworth discovered the potentially catastrophic problem of modal noise [1]. Modal noise in laser-based MMF links was recently more completely addressed and theoretical as well as experimental proofs showed that long-wavelength operation of MMF's is robust to modal noise [2], [3]. This explains the spectacular regain of interest for MMF's as the best solution for the cabling of LAN's. The question that needs answer now in view of increasing the usefulness of multimode fibers concerns the improvement of their dispersion characteristics. Because MMF's propagate a large number of modes having different velocities, they produce a signal response inferior to that of single-mode fibers. For standard 62.5/125 μm MMF's, the minimum bandwidths are only specified to be 200 and 500 MHz·km [4] in the 850 and 1300 nm transmission windows, respectively, under uniform overfilled-excitation condition [5]. Even though these specifications do satisfy the information rate of many classical short-range links, it is clear that a 2-km-long campus backbone cannot be realized for operation at the speed of gigabit Ethernet. Until wavelength-division-multiplexing (WDM) technology becomes available and inexpensive, the potential MMF capacity for digital communication needs a greater exploitation to meet user requirements for higher data rates and to support emerging multimedia applications. To enable the design and utilization of MMF's with such enhanced speeds, the development of an accurate bandwidth model is of prime importance. Through the dispersion modeling more likely performance limits can be established, thereby preventing eventual overdesign of systems and the resulting cost.

Since the mid-1970's, much work has been directed to the investigation of MMF's and their ability for high speed transmission. So far, different factors have clearly been identified to influence the information-carrying capacity, namely, the material dispersion (in combination with the spectrum of the exciting source) [6], [36], [7], the launching conditions [8], [9], as well as the mode-dependent characteristics (i.e., delay [6], [36] attenuation [10], and coupling-coefficient [10]–[12]). Unfortunately, the achievements, so far accomplished, are not quite complete to enable precise bandwidth prediction if an arbitrary operating condition is to

Manuscript received May 21, 1999; revised September 22, 1999. This work was done within the framework of the Dutch Research Project IOP Electro-Optics ongoing in the COBRA Research Institute, Eindhoven University of Technology.

The author is with COBRA, Interuniversity Research Institute, Eindhoven University of Technology, Eindhoven 5600 MB, The Netherlands.

Publisher Item Identifier S 0733-8724(00)01314-1.

be considered. To our knowledge, none of dispersion evaluation models reported in the previous literature incorporates the involved parameters together. This might explain, among others, why measured bandwidths in MMF's seldom match exactly with theory. The most interesting description of pulse broadening in graded-index (GRIN) MMF's was certainly that of Olshansky and Keck [6]. This dispersion model provided essential guidelines for the development of GRIN fibers. But because this theory treated only the particular case of uniform overfilled launching (EOFL), and additionally neglects the differential mode attenuation (DMA) as well as the mode-conversion, it needs reconsideration. The analysis of the mode-conversion was given in [12], but it ignores the DMA and no longer associates the contribution of material dispersion. Consequently, these results can efficiently be applied only at long enough transmission length under fiber operation at a zero width wavelength region. This is not practically the case since most MMF systems use broad-band sources such as light emitting diodes (LED's) or Fabry–Perot (FP) lasers. Recent publications are also referring to vertical-cavity surface-emitting lasers (VCSEL's). It is the purpose of the present work to give for the first time a more general approach to the analysis of the bandwidth. This model is based on aspects of the models developed in previous works, but includes most items involved in the determination of the aggregate dispersion. It can be used at any wavelength under any operating condition. Moreover, this study properly allows for a quantitative evaluation of the influence of the fiber geometry, which is an important figure of merit in relation to the ease of connecting and handling, as mentioned earlier.

The 3-dB bandwidth is analyzed through the study of the fiber transfer function which introduces the wavelength and modal effects as two separate filter functions. The formal derivation of the chromatic transfer function is analytical, while the modal transfer function is obtained by numerically solving the power flow equation in the frequency domain. To make it easy to use our theory for the description of any GRIN MMF, the general formalism is first displayed together with a careful presentation of the latent assumptions and approximations. Particular parameter-values are subsequently chosen for computer simulations based on studying samples of silica glass fibers fabricated by Plasma Optical Fiber. Illustrative results are reported with special focus spent on analyzing the influence of the fiber core and outer diameters.

II. Theory

The first transmission optical fibers consisted of a high refractive index core surrounded by a lower refractive index cladding. The index step between the core and cladding causes light to be trapped by total reflection at the core-to-cladding boundary. Within the requirement of a lower index for the cladding, the profile may in general take any form. However, the specific shape of the profile has a considerable effect on the distribution and the characteristics of the propagated light and therefrom influences the performance parameters of the fiber (dispersion, loss...). The power-law or so-called α-profile grading is of particular importance for minimized dispersion and has become commonly used at this purpose. Therefore, the multimode GRIN fibers whose dispersion will be examined here have a refractive index profile defined by

$$n(r,\lambda)=\begin{cases} n_1(\lambda)[1-2\Delta(\lambda)(r/a)^{\alpha}]^{1/2}, & \text{for } 0\le r\le a \\ n_1(\lambda)[1-2\Delta(\lambda)]^{1/2}, & \text{for } r\ge a \end{cases} \tag{1}$$

where

- r offset distance from the core center;
- λ free space wavelength of the fiber excitation light;
- α refractive index exponent $(\alpha>0)$;
- $n_1(\lambda)$ refractive index in the center of the core;
- $\Delta(\lambda)$ refractive index contrast between the core center and the cladding;
- a core radius (i.e., the radius at which the index $n(r,\lambda)$ reaches the cladding value $n_2(\lambda)=n_1(\lambda)[1-2\Delta(\lambda)]^{1/2}$.

It is to be noted that the core grading becomes parabolic for $\alpha=2$ and converges to the step-index profile (uniform core) for $\alpha=\infty$.

It is anticipated that the well-known Sellmeier equation will be used to evaluate both the refractive indices of the cladding and that of the core central region. This equation involves several parameters (known as Sellmeier constants) that are dependent on the dopant and its concentration. Because this relationship may present a certain degree of nonlinearity, it may not exactly be true that the index profile will obey (1) with a single α. This behavior is usually check by measuring the differential mode delay (DMD) as a function of the lateral displacement r. The results of these tests at 1300 nm supplied to us by the manufacturer shows one single optical region for the core. We confirmed this by achieving single-α fittings of (1) to measured index profiles on PCVD preforms. We believe that the circular symmetric profile as defined by (1) is a good representation of the refractive index. Nevertheless, it should be outlined that the index exponent α may slightly vary with wavelength, always due to the eventually nonlinear Sellmeier coefficients. As a consequence of this, a profile conceived to be optimal at a given wavelength, for example 1300 nm, may well be far from optimal at another wavelength, for example 850 nm. The α-dispersion is imposed by the dopant and its concentration, so this impairment is not easy to overcome. A possible solution would consist of implementing the so-called multiple-α index profiles as proposed in [13], but the fiber fabrication will become more complicated. This aspect of the investigation is not treated in this paper but could be the subject of a future analysis.

A. Formulation for Fiber Dispersion Analysis

Multimode optical fibers described by (1) support a large but finite number of modes which are particular solutions of the Maxwell's equations. Each mode propagates at its own velocity resulting from its particular propagation constant. From

the WKB analysis the modal propagation constant was approximately derived as [12]

$$\beta(m,\,\lambda) = 2\pi\,\frac{n_1(\lambda)}{\lambda}\left\{1 - 2\Delta(\lambda)\left[\frac{m}{M(\lambda)}\right]^{2\alpha/(\alpha+2)}\right\}^{1/2} \tag{2}$$

where m is the principal mode number and $M(\lambda)$ is the total number of mode groups given by

$$M(\lambda) = 2\pi a\,\frac{n_1(\lambda)}{\lambda}\,\left[\frac{\alpha\Delta(\lambda)}{\alpha+2}\right]^{1/2}. \tag{3}$$

The principal mode number (or mode group number) appearing in (2) is defined as $m = 2\mu + \nu + 1$, in which the parameters μ and ν are referred to as radial and azimuthal mode number, respectively. Physically, μ and ν have the meaning that they count the number of maximum intensities that may appear in the radial and azimuthal direction in the field intensities of a given mode. In a strict sense, the mode number m is a discrete integer parameter, which takes values ranging from unity to the total number of mode groups. However, very often m can be treated as a continuous variable. This approximation is of great interest because it allows one to replace the discrete mode spectrum by a modal continuum. As a result, the WKB method can readily be used and mode sums can be converted to integrals that are easier to handle. A mode-continuum theory was presented in [14] for parabolic-index fibers. In this analysis, the validity of the mode-continuum was essentially related to the spectral extent of the exciting source. In other words, the large number of guided modes generally believed to be the main condition seems actually not required but even only two of them may constitute a continuum. Here we will suppose the laser spectrum to have a Gaussian distribution of the form

$$P(\lambda,\,\lambda_0) = \frac{1}{\sigma_\lambda\sqrt{2\pi}}\,\exp[-(\lambda-\lambda_0)^2/(2\sigma_\lambda^2)] \tag{4}$$

where λ_0 is the central wavelength of the spectrum and σ_λ stands for the rms spectral linewidth. Following the approach of [14], we found that the condition for the validity of the continuum approximation for the more general power-law profiles defined by (1) is

$$\sigma_\lambda \geq \frac{\lambda_0^2}{\pi a N_1(\lambda_0)}\,\left[\frac{\alpha\Delta(\lambda_0)}{\alpha+2}\right]^{1/2}\left(\frac{m}{M_0}\right)^{(\alpha-2)/(\alpha+2)} \tag{5}$$

where $M_0 = M(\lambda_0)$ and $N_1(\lambda_0)$ is the material group index defined by $N_1(\lambda_0) = n_1(\lambda_0) - \lambda n_1'(\lambda_0)$ in which the prime means derivative with respect to wavelength.

To get a clear idea on whether (5) is or is not fulfilled under practical circumstances, a numerical example must be given. For a typical parabolic or a nearly parabolic-index fiber with $a = 30$ μm, $\lambda_0 = 1300$ nm, $\Delta(\lambda_0) = 0.01$, the minimum linewidth is found approximately to be 0.8 nm. This condition may fail in highly coherent transmission systems using quantum-well light sources, but should be largely satisfied in current multimode fiber links which mostly employ LED's or FP lasers. The linewidth for LED's is approximately 15 nm, which is comfortable. The linewidth for FP lasers and *a fortiori* that of emerging VCSEL's is located between 1 and 3 nm, which is also sufficient.

It must be recognized that little explanation was given in [14] about the basic concept that withstands the mode-continuum theory. More particularly, the authors did not specify whether their criterion should be viewed as a necessary and/or sufficient condition. Although the desired results are obtained here for the mode-continuum approximation to be applicable, we envisage to reconsider this subject in another paper. For now it is convenient if we carry out the present work within the assumption that guided modes in fiber form a continuum. We will implicitly suppose this throughout the rest of the development without giving any further explanation.

In a strict sense, a signal propagated through an optical fiber will inevitably be nonlinearly distorted to some extent [15]. In practice, both linear and nonlinear distortions will be present. This occurs in highly coherent systems, when the signal bandwidth is comparable to the source bandwidth or larger [16]. Here, we consider only the case of large enough linewidth sources and regard a multimode fiber characterized by the α-class index profile displayed in (1) as linear in its input-output power relationship [17]. In this condition, the ratio of the baseband spectra of the output and input light is signal-independent and is called the baseband power transfer function. It determines the degree to which the input signal can be linearly distorted during propagation. For SMF's, a formula of the baseband power transfer function was previously derived and can be expressed as [18], [19]

$$H_{\mathrm{SMF}}(\lambda_0,\,z,\,\omega) = \int_{-\infty}^{\infty} P(\lambda,\,\lambda_0)L(\lambda,\,z)\,\exp[-i\omega\tau(\lambda)z]\,d\lambda \tag{6}$$

where z is the length of fiber, ω the angular baseband frequency, $L(\lambda,\,z)$ is the fiber loss at position z, and $\tau(\lambda)$ is the propagation delay per unit length. Relation (6) is valid within the assumption that the electrical angular frequency ω is much smaller that the optical angular frequency Ω_0, and is also much smaller than the spectral frequency range $\Omega_0\sigma_\lambda/\lambda_0$. The first condition is largely fulfilled in actual communication systems. The second condition may equally be expected to be satisfied if the rms spectral width is as large as required for the validity of the mode-continuum approximation. It is of interest to precise that the power spectral density involved in (6) is not required to present a Gaussian shape, but it can *a priori* have any form. The only assumption behind $P(\lambda,\,\lambda_0)$ is that it should be time-independent.

Equation (6) can readily be modified and extended to the description of multimode fiber dispersion. In this case, we must introduce the light coupling efficiency, $C_{\mathrm{eff}}(m,\,\lambda)$, into each mode and also take into account the fact that both loss and delay now depend on modes. Subsequently, the result of this operation must be integrated in order to incorporate the contribution of all propagated modes. In so doing, we obtain

$$H_{\mathrm{MMF}}(\lambda_0,\,z,\,\omega) = \int_1^{M_0}\int_{-\infty}^{\infty} 2mP(\lambda,\,\lambda_0)C_{\mathrm{eff}}(m,\,\lambda)G(m,\,\lambda,\,z,\,\omega)$$

$$\times L(m, \lambda, z) \exp[-i\omega\tau(m, \lambda)z]\, d\lambda\, dm \tag{7}$$

where $\tau(m, \lambda)$ is the modal delay per unit length, $L(m, \lambda, z)$ is the modal loss, the factor $2m$ denotes the degeneracy of level m and the function $G(m, \lambda, z, \omega)$ is arbitrary introduced to account for the mode mixing effect.

To evaluate (7), we will consider that the dependence on wavelength of three modal quantities, namely, the launching efficiency, the mode-mixing function as well as the distributed loss is negligible in the transmission window of interest. Within this simplifying assumption, which should be fairly realistic in practice, $C_{\text{eff}}(m, \lambda)$, $G(m, \lambda, z, \omega)$, and $L(m, \lambda, z)$ can be approximated by their respective values at the central wavelength λ_0. Because the modal delay time $\tau(m, \lambda)$ is more sensitive to the dependence of the refractive index with wavelength, it is more accurately assessed by a Taylor series expansion, i.e.,

$$\begin{aligned}\tau(m, \lambda) = &\tau(m, \lambda_0) + D(m, \lambda_0)(\lambda - \lambda_0) \\ &+ \tfrac{1}{2} S(m, \lambda_0)(\lambda - \lambda_0)^2 + \cdots\end{aligned} \tag{8}$$

where $D(m, \lambda_0) = \tau'(m, \lambda_0)$ is, by definition, the chromatic dispersion of mode m, and $S(m, \lambda_0) = \tau''(m, \lambda_0)$ can be defined as the modal dispersion slope. Note that the condition for (8) to be valid is $\sigma_\lambda/(2\lambda_0) \ll 1$, which is largely satisfied even for broadband LED's. Substituting (8) into (7) and assuming that $D(m, \lambda_0)$ and $S(m, \lambda_0)$ can be, respectively, replaced by averaged values $D_0(\lambda_0)$ and $S_0(\lambda_0)$, yields

$$H_{\text{MMF}}(\lambda_0, z, \omega) = H_{\text{chromatic}}(\lambda_0, z, \omega) H_{\text{modal}}(\lambda_0, z, \omega) \tag{9}$$

with

$$\begin{aligned}&H_{\text{chromatic}}(\lambda_0, z, \omega) \\ &\quad = \int_{-\infty}^{\infty} P(\lambda, \lambda_0) \exp\{-i\omega z[D_0(\lambda_0)(\lambda - \lambda_0) \\ &\qquad + \tfrac{1}{2} S_0(\lambda_0)(\lambda - \lambda_0)^2]\}\, d\lambda\end{aligned} \tag{10}$$

$$\begin{aligned}&H_{\text{modal}}(\lambda_0, z, \omega) \\ &\quad = \int_1^{M_0} 2mC_{\text{eff}}(m, \lambda_0) G(m, \lambda_0, z, \omega) L(m, \lambda_0, z) \\ &\qquad \cdot \exp[-i\omega\tau(m, \lambda_0)z]\, dm.\end{aligned} \tag{11}$$

Relations (9)–(11) show that the transfer function of multimode fibers can be modeled by a product of two filter functions $H_{\text{chromatic}}(\lambda_0, z, \omega)$ and $H_{\text{modal}}(\lambda_0, z, \omega)$ describing the chromatic and intermodal dispersions. Equation (9) additionally expresses the latent idea that the two capacity-limiting factors can be considered as independent effects despite the mode-coupling. The chromatic part results from the fact that the delay time of each propagated mode depends on wavelength. The modal part, however, depends on less controlled variables. Indeed, observation of (11) shows that the excitation conditions, difference in delays among the modes, the distributed loss as well as the power mixing between modes are simultaneously involved in the determination the intermodal dispersion. It seems convenient to refer $H_{\text{chromatic}}(\lambda_0, z, \omega)$ and $H_{\text{modal}}(\lambda_0, z, \omega)$ to as chromatic and modal transfer functions, respectively, and discuss both separately.

B. Chromatic transfer function

The power spectral density $P(\lambda, \lambda_0)$ of the exciting source has to be specified to proceed to the derivation of the chromatic transfer function as defined in (10). Of course, for an arbitrary spectral shape the integral can only be handled numerically. Fortunately, it turns out that most of injection-lasers used in optical fiber communications have a Gaussian lineshape of the form given in (4) [20]. Using this type of distribution, the integral (10) can be calculated exactly. In general, the spectrum of current VCSEL's departs more or less from a Gaussian shape. Therefore, it seems more prudent to have recourse to the numerical integration for accurate bandwidth assessment in VCSEL-based MMF systems. The solution of (10) for the perfectly Gaussian linewidth case is [19], [21]

$$\begin{aligned}&H_{\text{chromatic}}(\lambda_0, z, \omega) \\ &\quad = \frac{1}{(1 + i\omega/\omega_2)^{1/2}} \exp\left[-\frac{(\omega/\omega_1)^2}{2(1 + i\omega/\omega_2)}\right]\end{aligned} \tag{12}$$

in which ω_1 and ω_2 have been introduced as abbreviations for

$$\omega_1 = -[\sigma_\lambda D_0(\lambda_0) z]^{-1} \tag{13}$$

$$\omega_2 = \{\sigma_\lambda^2[S_0(\lambda_0) + 2D_0(\lambda_0)/\lambda_0]z\}^{-1}. \tag{14}$$

Relations (12)–(14) are the same as those describing chromatic dispersion in single-mode fibers (SMF's) except that the material dispersion $D_0(\lambda_0)$ and the dispersion slope $S_0(\lambda_0)$ have to be considered as averaged quantities which include the contribution of each propagated mode. We have to mention, however, that, after computation, we have not recorded any significant difference between these averaged values compared to the usual material dispersion and dispersion slope. This appears to be a general result within the weak guidance rule ($\Delta \ll 1$), which *a posteriori* demonstrates the validity of our assumptions. Another comment that should be made from (12) to (14) is that for a fiber operated at a zero material dispersion wavelength, the chromatic contribution to bandwidth is not necessarily negligible because of the presence of the dispersion slope. Therefore, this term cannot systematically be ignored. It should be mentioned that when operating far from the zero dispersion region, in particular at wavelength like 850 nm, ω_2 is much larger than $|\omega_1|$ and (12) can be simplified into $\exp[-(\omega/\omega_1)^2/2]$, which means that the contribution of the dispersion slope [i.e., $S_0(\lambda_0)$ term in (10)], is negligible.

C. Modal Transfer Function

The modal transfer function described by (11) can also be written as

$$H_{\text{modal}}(\lambda_0, z, \omega) = \int_{x_0}^{1} 2xR(x, \lambda_0, z, \omega)\, dx \tag{15}$$

with

$$R(x, \lambda_0, z, \omega) = C_{\text{eff}}(x, \lambda_0)G(x, \lambda_0, z, \omega)L(x, \lambda_0, z) \cdot \exp[-i\omega\tau(x, \lambda_0)z] \quad (16)$$

where the normalized mode group number $x = m/M_0$ has been introduced and $x_0 = 1/M_0$. It is worth noting that the modal loss appearing in (16) as well as in (7) and (11) can be approximated by $L(x, \lambda_0, z) = \exp[-\gamma_T(x, \lambda_0)z]$ in which $\gamma_T(x, \lambda_0)$ stands for the total modal attenuation.

The function $R(x, \lambda_0, z, \omega)$ defined by (16) can be viewed as the modal power in Fourier domain. Unfortunately, (16) is unusable as it stands because if quantities such as the modal excitation efficiency, modal loss and modal delay can be estimated using WKB analysis, we know little about the so-called mode-mixing function. By assuming that the mode-conversion effect is negligible for distances much shorter than the coupling length L_c (i.e., length from which mode-coupling begins to impact the propagation [12]), the condition $G(x, \lambda_0, z, \omega) = 1$ (with $z \ll L_c$) must be imposed. Another assumption that can be reasonably made is that the temporal power distribution of each guided mode has a Gaussian shape. This follows from the preliminary hypothesis that nonlinear effects are negligible. In this case, the impulse response of a given mode should reflect the input Gaussian pulse but which is uniformly broadened due to chromatic dispersion. Owing to the properties of Fourier transforms, the mode-mixing function for an arbitrary z is Gaussian in turn, and can be expressed as $G(x, \lambda_0, z, \omega) = \exp[-\omega^2/(2\sigma_\omega)]$ with $\sigma_\omega = \sigma_\omega(x, \lambda_0, z)$. This is for now the maximum knowledge we can have about $G(x, \lambda_0, 0, \omega)$. Because the width σ_ω is essentially unknown, the formal calculation of formula (15) cannot be achieved by the aid of (16), at least if account has to be taken of the mode-conversion process. Fortunately, there exists an alternative way of evaluating the modal power. The power flow in propagated modes is best described by the following partial differential equation incorporating not only modal velocities, but also distributed loss and mode-conversion effects [12], [22]

$$\frac{\partial R(x, \lambda_0, z, \omega)}{\partial z} = -[i\omega\tau(x, \lambda_0) + \gamma(x, \lambda_0)]R(x, \lambda_0, z, \omega) + \frac{1}{x}\frac{\partial}{\partial x}\left[xd(x, \lambda_0)\frac{\partial R(x, \lambda_0, z, \omega)}{\partial x}\right] \quad (17)$$

where $d(x, \lambda_0)$ is the mode coupling coefficient normalized to M_0^2, and $\gamma(x, \lambda_0)$ is the modal attenuation (in the absence of coupling effect). We will suppose the total power at position z to be normalized such a way that

$$\int_{x_0}^{1} 2xR(x, \lambda_0, z, 0)\,dx = 1. \quad (18)$$

Equation (17) is in principle invalid when the mode parameter x reaches its extremities corresponding to the lowest and highest order modes. These are described by the so-called boundary conditions that will be specified further. Let us now discuss the mode-dependent parameters, i.e., modal delay, modal attenuation and mode-coupling coefficient, before proceeding to the solution of (17).

1) Modal Delay: The delay time of the guided modes can be derived from (2) using the definition $\tau(x, \lambda) = -\lambda^2\beta'(x, \lambda)/(2\pi C)$ where C is the speed of light in vacuum. The calculation yields approximately

$$\tau(x, \lambda) = \frac{N_1(\lambda)}{c}\left[1 - \frac{\Delta(\lambda)[4 + \epsilon(\lambda)]}{\alpha + 2}x^{2\alpha/(\alpha+2)}\right] \cdot [1 - 2\Delta(\lambda)x^{2\alpha/(\alpha+2)}]^{-1/2} \quad (19)$$

in which $\epsilon(\lambda)$ is the profile dispersion parameter given by

$$\epsilon(\lambda) = \frac{-2n_1(\lambda)}{N_1(\lambda)}\frac{\lambda\Delta'(\lambda)}{\Delta(\lambda)}. \quad (20)$$

2) Modal Attenuation: Modal attenuation originates from conventional loss mechanisms that are present in a usual fiber, that is, absorption [23], Rayleigh scattering [10], [23] and loss on reflection at the core-cladding interface [24]. These different loss mechanisms act on each mode in a different manner, which causes the attenuation coefficient to vary from mode to mode. For example the fiber boundary has a strong effect on modes near cut-off but little on the fundamental ones. But, contrary to what can be thought, the lower-order modes have not necessarily the slowest attenuation, in the general case. Indeed, the measurements show that the mode-dependent attenuation as a function of normalized mode number x exhibits a minimum which is sometimes shifted from the origin [23]. This occurs when the dopant material whose concentration is higher in the fiber center is highly scattering or absorbing. However, the results reported in [23] indicate that if the numerical aperture is small enough or if a long wavelength is used, in which case the scattering effect is minimized, the MDA is gradually increasing.

In a strict sense, a proper model for each of the main loss mechanisms mentioned above is required to accurately describe the MDA. This is not an easy task, the more so as such models will inevitably introduce a certain number of parameters which may be difficult to put on correct numerical values. We believe that as it is a common practice to systematically measure a fiber attenuation in the standard transmission windows, it should be the same for the MDA since it appears to have a strong effect on the characteristics. Such measured data could readily be incorporated in the simulation of the fiber characteristics by fitting an appropriate function. Since silica glass fibers are used on the long wavelength side around 850, 1300, and 1550 nm, for which the MDA should be increasing with increased mode order, we suggest to use the following functional form:

$$\gamma(x, \lambda) = \gamma_0(\lambda) + \gamma_0(\lambda)I_\rho[\eta(x - x_0)^{2\alpha/(\alpha+2)}], \quad (21)$$

where $\gamma_0(\lambda)$ is the attenuation of low-order modes (i.e., intrinsic fiber attenuation), I_ρ is the ρth-order modified Bessel function of the first kind, and η is a weighting constant. This empirical formula has been set up by noticing that most measured MDA data displayed in the literature for long wavelengths conform to the shape of modified Bessel functions, but the particular form of the function does not matter here provided that it can be made suitable for fitting the measurements. Let us precise that it is the

difference in modal attenuation (i.e., differential mode attenuation, DMA) that determines the impact of distributed loss on fiber dispersion. The first term in (21) leads to an overall factor $\exp[-g_0(\lambda)z]$ to the solution and can be ignored in frequency response simulations. It is also worth mentioning that during propagation, modes with fastest power loss may be stripped off or attenuated so strongly that they no longer significantly contribute to the dispersion. In other words, the differential mode attenuation is a filtering effect, which may yield a certain bandwidth enhancement depending on the launch conditions and the transmission length.

3) Mode Coupling: Cross-coupling among guided modes in MMF's may result from internal as well as external causes. Internal sources of mode-coupling include imperfections such as core noncircularity [25] and refractive index fluctuations [26] caused by preform fabrication and fiber drawing process. In principle, mode-mixing from core diameter variations should be negligible because perturbations due to the fiber fabrication process extend over many centimeters so that the phase matching condition is unsatisfied for power transfer between modes belonging to different mode groups. On the other hand, because in this paper we deal with modern silica glass fibers made on using the high-performance PCVD method, we will also neglect the effect of refractive index variations and consider only external perturbations to be the most dominant source of coupling. This is the case whenever fibers are used such a way that they are subjected to external forces. This may occur whether from coating, cabling, packaging, storage drums, etc. Fiber winding on drum, for example, forces the fiber to partially conform to the crookedness of the drum surface, which give rise to small deformations (microbends) that cause the coupling. An interesting and valuable study of this subject was previously presented by Olshansky [12], [27]. We adopt here the same analysis together with the selection rules of neighboring mode group approximation, but we modify the form of the curvature spectrum to include the fiber external diameter. In so doing, we found the following functional expression for the normalized mode-coupling coefficient:

$$d(x,\lambda) = C_s \left(\frac{h}{b}\right)^p \left(\frac{a}{b}\right)^{2p} \left[\frac{\alpha+2}{\alpha\Delta(\lambda)}\right]^{1+p} x^{-2q} \qquad (22)$$

with

$$q = [p(\alpha-2)-2]/(\alpha+2), \qquad (23)$$

where C_s can be labeled mode-coupling constant, h is the rms height of the deformation, b is the total fiber radius, p is a fitting parameter introduced in the purpose of covering a large range of sources of perturbations. It is worth mentioning that the index fluctuations could be included without altering the basic structure of the model. As indicated above, the fluctuations of the refractive index can be regarded as an extra mode-coupling source [26], likewise only (22) needs be properly modified. The problem is that this will inevitably introduce new parameters whose numerical values would be difficult to find. As a matter of fact, there is for instant no practical way of separating the index fluctuations from the microbending effects. Because the measured refractive index profiles supplied to us by the manufacturer show smooth contours with no particular defects such as dips or peaks we believe that the index fluctuations can be neglected here as an approximation. However, it is worth noticing that since the numerical value of the coupling constant C_s will be deduced from a fitting procedure of a measured attenuation, an eventual presence of nonconsidered source of perturbation will partially be corrected.

Inspection of (22) indicates that there is a significant difference in the mode conversion coefficient between step-index fibers and parabolic or nearly parabolic-index fibers. We see that for $\alpha = 2$ the mode-coupling coefficient increases linearly with mode order x, while it reduces as x^{-2p} for $\alpha = \infty$. This means that in nearly parabolic-index fibers, higher-order modes have the greater sensitivity to microbending than lower-order ones, but the situation is reversed in step-index fibers. This is the reason why these generally show stronger mode-mixing effect than the graded-index type because, owing the fast attenuation of high-order modes, they are stripped off during propagation, or are not excited at all as in low-numerical-aperture launch systems. It should be mentioned that the different behavior between SI and GI fibers with regard to microbending was previously confirmed by experiment [28]. But, because the refractive index is never perfectly parabolic in GI fibers, the measured coupling coefficient versus mode group number slightly departs from a linear characteristic.

A number of interesting implications can be foreseen from (22) regarding fiber design and practical utilization. Indeed, the mode-coupling coefficient is seen to depend strongly on the fiber core radius a, the fiber outer radius b, and the refractive index contrast $\Delta(\lambda)$. These parameters thus suggest three possible ways of designing fibers with high or low susceptibility to mode-coupling from microbends. An increase of the core diameter and a reduction in the outer diameter or the numerical aperture will increase the strength of the coupling. The influence of the core diameter [24] and that of the numerical aperture [29] have been qualitatively verified. Formula (22) also indicates that if one considers different fibers drawn from the same preform such a way that the ratio between the core and outer diameters remains constant, the thin one will be more sensitive to microbends and are expected to exhibit higher bandwidth. However, one must be careful when acting on a fiber geometry to gain more bandwidth by mode mixing. Indeed, the presence of mixing means not only power flow among guided modes during propagation, but also power transfer from guided to unguided modes causing extra loss. On the other hand, reducing the index contrast will increase the difficulty of obtaining low-loss interconnection of cable segments and also will reduce the fiber's ability of gathering light, in particular if the light source is incoherent. These coupling loss penalties which are expected to increase with the strength of coupling must be weighted with the benefit of enhanced bandwidth.

4) Numerical Method: Now that the forms of the functions $\gamma(x,\lambda)$, $\tau(x,\lambda)$, and $d(x,\lambda)$ are known, one can proceed to the solution of the power flow equation. It should be mentioned that in certain simplified cases it can be solved exactly [11], [12]. In the more general situation where all the parameters are mode-dependent, no simple analytical solutions are available

and the modal transfer characteristics can be obtained only using a numerical procedure. The numerical integration consists of discretizing the x and z variables to form a rectangular lattice. At each point (i, k) of the grid the derivatives are approximated by an appropriate finite difference which determines the choice of method. A variety of such schemes are given in the literature. Here, we will adopt the Crank–Nicholson implicit procedure which yields a stable solution that converges more rapidly than ordinary difference methods. Our choice for Crank–Nicholson scheme is additionally motivated by the fact that this method has already been successfully applied to fibers [30]–[32].

Let h_x and h_z be the segmentation steps of the variables x and z, respectively. The power flow equation with $R(x, \lambda_0, z, \omega)$ can be replaced by a set of finite-difference equations with $R_{j,k} = R(x_j, \lambda_0, z_k, \omega)$ where $x_j = x_0 + jh_x$ and $z_k = kh_z$. By applying the Crank–Nicholson implicit scheme to (17), it is transformed into

$$\frac{R_{j,k+1} - R_{j,k}}{h_z} = \frac{U_{j,k} + U_{j,k+1}}{2} \tag{24}$$

where $U_{j,k}$ is the discretized form of the right hand side of (17), obtained by using ordinary numerical differentiation formulas. The calculation leads to the following relationship:

$$\begin{aligned} A_j R_{j-1,k+1} + B_j R_{j,k+1} + C_j R_{j+1,k+1} \\ = D_j R_{j-1,k} + E_j R_{j,k} + F_j R_{j+1,k} \end{aligned} \tag{25}$$

with

$$\begin{cases} A_j = -h_z d_j / h_x^2 \\ B_j = 2 + h_z(i\omega\tau_j + \gamma_j) + h_z(x_{j+1}d_{j+1} + x_j d_j)/(x_j h_x^2) \\ C_j = -h_z x_{j+1} d_{j+1}/(x_j h_x^2) \\ D_j = -A_j \\ E_j = 2 - h_z(i\omega\tau_j + \gamma_j) - h_z(x_{j+1}d_{j+1} + x_j d_j)/(x_j h_x^2) \\ F_j = -C_j \end{cases} \tag{26}$$

where

$$\begin{cases} d_j = d(x_j, \lambda_0) \\ \tau_j = \tau(x_j, \lambda_0) \\ \gamma_j = \gamma(x_j, \lambda_0). \end{cases} \tag{27}$$

The unknowns $R_{j,k}$ can be computed from (25) and employed in the determination of the modal transfer function by approximating (15) by any numerical integration method. We will use Simpson's rule in the present analysis. It should be mentioned, in passing, that once the $R_{j,k}$ are known, the mode-mixing function as defined in (16) can be tabulated, but this is out of the scope of this work.

For the computation of (25), initial and boundary conditions have to be specified. A variety of light-coupling methods can be applied to multimode fibers [8], [9]. As a general rule, the mode excitation can be simulated by computing the launching efficiency as overlap integral of the electrical field of each fiber mode with the electrical field of the incident light ("overlap integral method"). But, although the numerical model presented here has been developed for any excitation, we will restrict ourselves to the case of overfilled launching (OFL) with equal power coupled into each mode at the input end of the fiber. Within this consideration, the initial power distribution $R_{j,0}$, which is equivalent to the launching efficiency $C_{\text{eff}}(x_j, \lambda_0)$, can be formally set to unity for each mode. The advantage of the full excitation over restricted launching is that the large number of propagating modes provides a better modal noise immunity [2]. The reader is to be aware that the uniform OFL assumption should be fairly realistic when using LED-based transmitters but it should be viewed as an approximation for laser- and VCSEL-based systems. In both cases the overlap integral method should be used for more accuracy.

The boundary conditions are chosen as follows. To determine the highest boundary condition, we consider that leaky modes do not transport significant power, which should be a realistic assumption, i.e.

$$R(x, \lambda_0, z, \omega) = 0 \qquad \text{for } x > 1. \tag{28}$$

The lowest boundary condition is more difficult to establish. It was often derived by considering that the lowest-order modes are unsubjected to coupling-induced losses [12]. This criterion can be a good approximation under full launching with equal power coupled into modes, but it may be rough or even may not hold true in a number of cases including, for example, when only the fundamental modes are being excited. We will refine this boundary model and describe the fundamental modes by their own propagation equation given as

$$\begin{aligned} \frac{\partial R(x_0, \lambda_0, z, \omega)}{\partial z} = &-(i\omega\tau_0 + \gamma_0) R(x_0, \lambda_0, z, \omega) \\ &+ M_0 d_0 \left[\frac{\partial R(x, \lambda_0, z, \omega)}{\partial x}\right]_{x=x_0}. \end{aligned} \tag{29}$$

III. Results and Discussion

We will analyze the dispersion characteristics of ternary graded-index fibers with a GeO_2–F–SiO_2 core and a F–SiO_2 cladding. These fibers are fabricated by Plasma Optical Fiber by the high-performance PCVD method. A small amount of fluorine (0.04 mol-%) is uniformly doped over the core and cladding regions. The core center has a 13.5 mol-% of germanium which is gradually decreased in the lateral direction to form the desired grading. These MMF's exhibit a numerical aperture (NA) of nearly 0.2. On the other hand, their refractive index profile shows a smooth shape (i.e., no dips or peaks) and can be approximated with a single α-factor varying between 1.9 and 2.02. To enable computer evaluations, it is assumed that the refractive indices of the core and cladding materials follow three-term Sellmeier functions of wavelength [33]. For the 3-dBo bandwidth prediction, an exciting source of rms spectral width of $\sigma_\lambda = 3$ nm is considered. Of course, the parameters of both the distributed loss and mode-coupling must be specified, as well. The functional expression of the modal attenuation is fitted to the measurements presented in [30] for $\rho = 9$ and $\eta = 7.35$. The resulting plot is reported in Fig. 1 showing that the proposed MDA fitting function is quite appropriate. As indicated earlier, the mode-coupling parameters (p, h, and Cs) depend on the nature of the perturbation source that gives rise to the power conversion. Here, we deal with nylon-coated fibers that are classically wound in

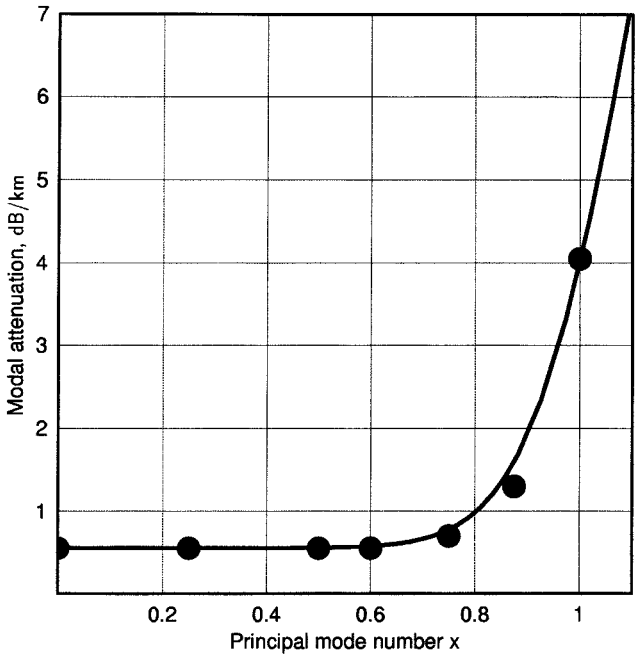

Fig. 1. Mode-dependent attenuation (MDA) as a function of normalized mode order x: The dots represent the measurements of [31], while the solid curve is the fitted MDA formula (21) with $\rho = 9$ and $\eta = 7.35$. Note that the curve is slightly shifted vertically according to the common attenuation of 0.55 dB/km that we measured.

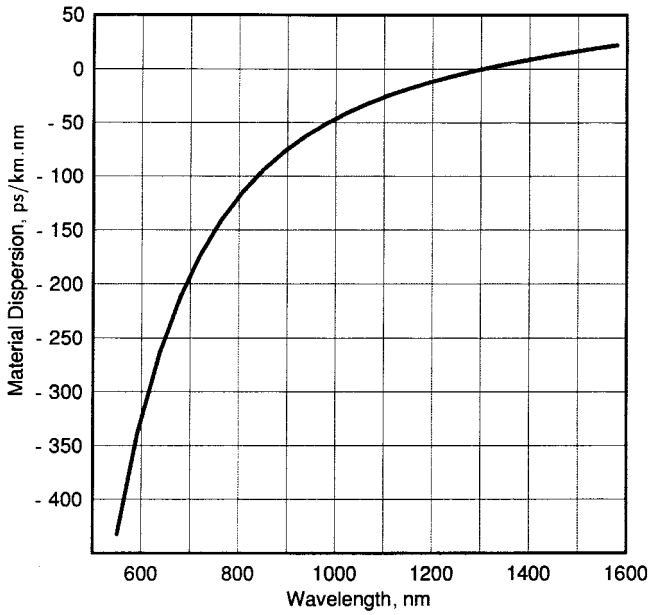

Fig. 2. Material dispersion of the core as a function of wavelength [33].

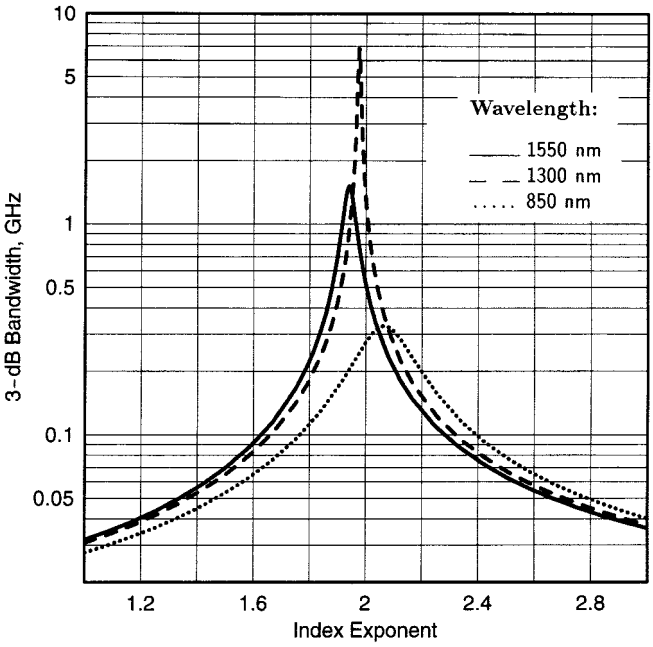

Fig. 3. 3-dBo baseband bandwidth of a 2014-m-long fiber as a function of refractive index exponent for wavelengths $\lambda_0 = 850, 1300,$ and 1550 nm. All three curves are based on the results of analysis presented in [6].

one layer on 30 cm-diameter supporting drums. It is therefore reasonable to adopt Olshansky's assumptions [26] and choose $p = 2$. Further on, we formally set h to 1 μm, and evaluate the coupling constant by fitting the theoretical attenuation with the measurement. We obtained $Cs = 6 \times 10^{-5}$ km^{-1} which yields for a 93/125 μm fiber operated at a 1300 nm wavelength, a predicted attenuation of 1.24 dB/km. This result was recorded at a transmission length of 2014 m and is in agreement with the measured value supplied by Plasma Optical Fiber. As can be noticed some of the parameters have been estimated by reference to data from twenty years ago that may be suspected as too old sources. During the simulations, we have verified that the modal attenuation and mode coupling are not extremely sensitive phenomena but can reduce or strengthen to some degree without greatly altering the dispersion. For this reason, we believe that the above numerical values should apply to a wide range of fibers including our modern samples.

The dispersion of the fibers core material is reported in Fig. 2. The result shows a zero crossing around 1300 nm, so in this region the chromatic dispersion effect should not be significant and the 3-dBo bandwidth should be mostly affected by intermodal dispersion. This is the reason why the 1300 nm-wavelength region is particularly attractive, the more so as it corresponds to a local minimum in the fiber loss versus wavelength curve. At the two remaining low-loss transmission windows of 850 and 1550 nm, the material dispersion is seen to be as high as -94 and 20 ps/nm·km, respectively. Therefore at 850 and 1550 nm, the bandwidth will be affected not only by intermodal dispersion but also by chromatic dispersion, more or less strongly depending on the spectral extent of the driving source. To qualitatively confirm this, the 3-dBo bandwidths are reported in Fig. 3 as functions of the refractive index exponent for the three standard wavelengths. These plots are based on Olshansky and Keck's theory which neglects distributed attenuation and mode-coupling effects [6]. The characteristic feature of the grading is the well-known peaked bandwidth due to intermodal dispersion. With our choice of parameter-values, the maxima are located around α-factors of 2.06, 1.97, and 1.94, for 850, 1300, and 1550 nm wavelengths, respectively. By implementing these optimum values in the fiber-core grading, the intermodal dispersion will be minimized and the peak height will be governed mostly by chromatic dispersion.

In an attempt to assess the accuracy of the numerical calculation, a series of frequency response

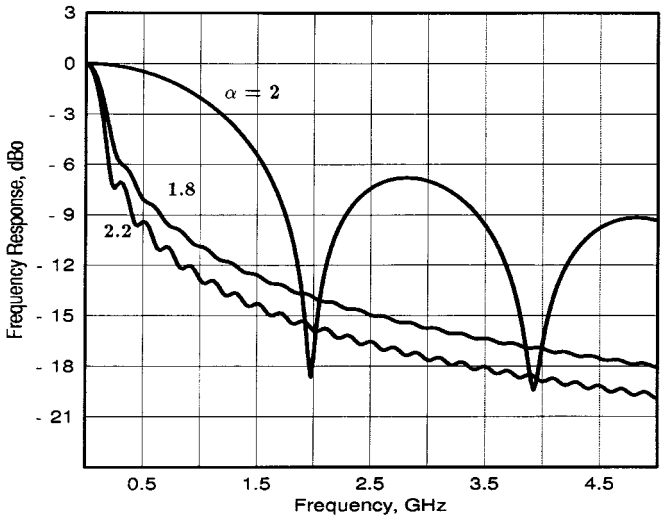

Fig. 4. Frequency responses for a 2014-m-long fiber with $\lambda_0 = 1300$ nm and varying index exponent of $\alpha = 1.8, 2, 2.2$. These results are based on the present analysis in which distributed loss and mode-coupling effects are neglected.

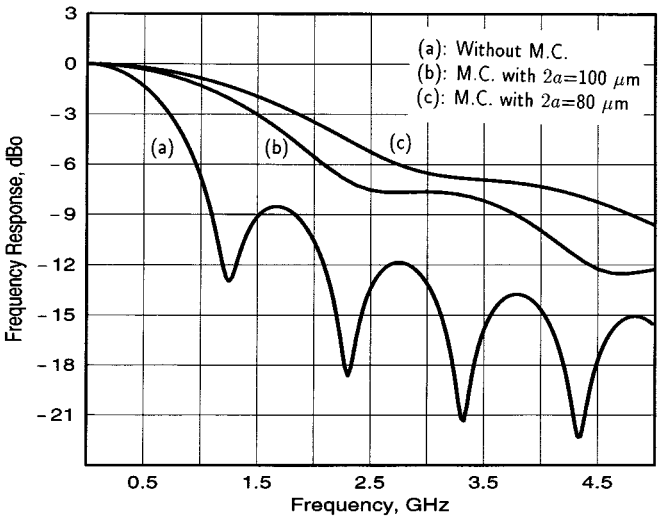

Fig. 5. Influence of the core diameter on the frequency response at $\lambda_0 = 1300$ nm for a 2014-m-long fiber with fixed ratio between the core and outer diameters ($a/b = 0.8$).

$[10 \log_{10}(|H_{\mathrm{MMF}}(\lambda_0, z, \omega)|)]$ simulations has been carried out without including the differential attenuation and mode-coupling effects. Some of these results are displayed in Fig. 4 for wavelengths of 1300 nm and for varying index exponent of 1.8, 2, and 2.4. The corresponding curves indicate 3-dBo baseband bandwidths of 183, 1200, and 150 MHz, respectively. These numbers exactly match with those obtained using Olshansky and Keck's theory as displayed in Fig. 3, except in the case $\alpha = 2$ for which Olshansky and Keck's analysis gives 1279 MHz instead of 1200 MHz. We believe that this slight discrepancy is to be connected to the approximations made by Olshansky and Keck, rather than being a cause of an eventual inaccuracy of the present model. As a matter of fact, the results given in [6] neglect a term proportional to the square spectral width in the intermodal dispersion formula. This term which is the source contribution to intermodal dispersion is quite small when the first term in (25) of [6] is high enough, but it becomes significant for refractive index exponents approaching the optimum value.

Frequency responses are displayed in Figs. 5 and 6 showing the influence of the fiber core diameter. The index exponent is taken to be 2.02 and will be maintained to the same value in all subsequent simulations. Curves in Fig. 6 are plotted for a fixed outside diameter, whereas results in Fig. 5 are obtained for a constant ratio between the core and outside diameters. For comparison a curve is reported in Fig. 5 representing the frequency response predicted when the fiber's operation is coupling-free. As a general rule, the two figures confirm that more bandwidth can be gained by mode-coupling. This principle follows from the fact that the mixing process forces the total light energy to propagate at an average speed [34]. Since no extra mode is excited during propagation, the average speed is less than without coupling, which explains the reduction of the modal dispersion. Fig. 5 shows that when the core/cladding diameter ratio (i.e., a/b) is maintained to a fixed value, the baseband

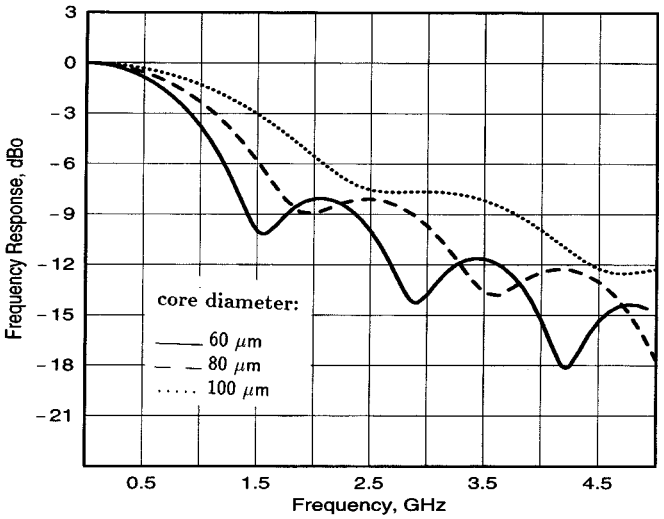

Fig. 6. Influence of the core diameter on the frequency response at $\lambda_0 = 1300$ nm for a 2014-m-long fiber with fixed outside diameter $2b = 125$ μm.

bandwidth diminishes with an increasing core diameter. On the other hand, in the case of fixed outer diameter (Fig. 6), an increasing core diameter improves the bandwidth. These trends agree well with (21) from which the coupling is seen to become more or less stronger depending on how the core and outer diameters are varied. It should be noticed that the bandwidth can substantially be increased through the mode-mixing effect. For a 80/125-μm fiber, for example, the frequency responses (see Fig. 5) indicate a 3-dB bandwidth of 725 MHz under mixing-free operation against 1900 MHz in the presence of mode mixing. This roughly corresponds to a threefold enhancement. In other words, the fiber geometrical dimensions provide a possible method of designing fibers with a potentially-large capacity for digital transmission. However, as already mentioned, the benefit of enhanced bandwidth must be

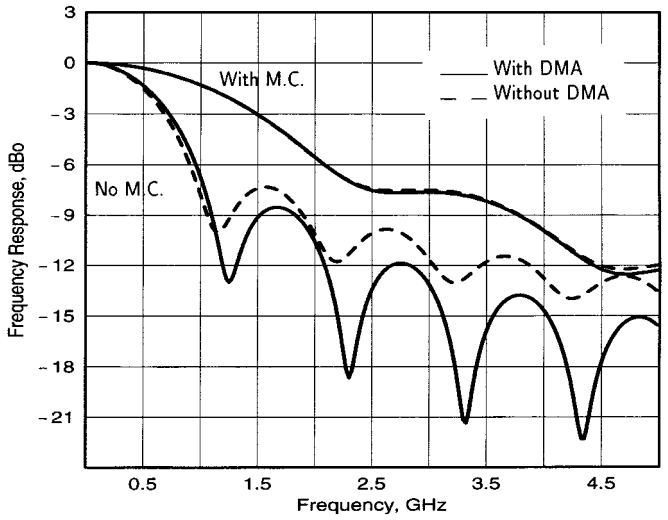

Fig. 7. Frequency responses of a 80/125 μm fiber showing the effect of differential mode attenuation (DMA) in presence and in absence of mode-coupling (M.C.): $\lambda_0 = 1300$ nm, $z = 2014$ m.

weighted with the extra power penalty caused by a strong mode-mixing. The reader must also be advised that international standards and the need to be compatible with the existing infrastructure may put some constraints on the choice of the fiber dimensions.

Finally, we have reported frequency responses in Fig. 7 showing the influence of the differential mode attenuation in absence and in presence of mode-coupling. It is shown that the DMA has little effect on the bandwidth itself, at least over the length of fiber considered here. The frequency responses, however, appear to be affected to a certain degree on the high-frequency side. This effect is seen to be more or less significant depending on whether the mode-mixing phenomenon is or is not involved. This different behavior can be easily understood in connection with the fact that in the presence of mixing the filtering effect of the DMA is held up due to infrequent coupling of energy into modes that might have been lost otherwise.

It is convenient to end the above discussion by a general and important observation from the frequency response simulations. It can be noticed that the curves do not roll off monotonously from the zero-frequency value but show a number of bumps whose amplitudes are relatively constant over a certain range of frequency. These bumps appear above the 3-dB cutoff frequency and are likely to present more pronounced and broadened heights in the absence of mode-mixing. These waves are seemingly not numerical artifacts since similar results were recorded in the measurements on fiber samples of 4.4 km in length [35]. The comparison of these experiments with theory will be reported later when all the parameter-values required in the simulations will become available to us. For now the following important comment can be made. Obviously, the bump regions cannot be included in the transmission bandwidth of single large-band channels owing to the strong attenuation with respect to the zero-frequency level. However, some of them are large and flat enough to allow for the transmission of passband channels, such as formed in subcarrier multiplexing (SCM) systems. These passband channels could be mixed together with the baseband signal in order to increase the data transmission capacity. This can be developed into a veritable technique for achieving the performance of gigabit Ethernet while still operating under overfilled launching. This finding brings more about the interest of determining the transfer function instead of directly calculating the bandwidth from the moments of the impulse response. From the present analysis, the existence of frequency ranges suitable for passband modulation are demonstrated. Unfortunately, the results are seen to depend on fiber dimensions as well as all items that affect the frequency response as described earlier. The most unpredictable parameter in the field is certainly the mode-mixing because the microbend pattern is susceptible of changing due to a change in external conditions. But, this problem can be prevented by adaptive allocation of the passband channels.

IV. Conclusion

The dispersion behavior of graded-index optical fibers is theoretically described including both chromatic and modal dispersions. We have shown that, within some reasonable conditions that should remain satisfied under usual circumstances, the two sources of dispersion can be considered to be independent effects. Accordingly, the transfer function has been separated into two parts regarded as chromatic and modal frequency responses. By assuming that the potential driving source has a Gaussian spectrum, the chromatic transfer function is derived analytically, while the modal transfer function is obtained on numerically solving the power flow equation incorporating distributed loss and mode-conversion process.

Frequency responses are reported which are mainly focused on the analysis of the influence of the fiber geometry. The simulation results show that an increased core diameter may reduce or increase the strength of mode-coupling depending on the relative values of the core and outside diameters. Considering fibers having different core diameters but similar core/cladding ratio (which is the case if they are drawn from the same type of PCVD preform), the analysis predicts the thick ones to be less susceptible to mode-coupling from microbends, leading to less bandwidth under overfilled launching condition. On the other hand, if the fiber size is maintained constant, an increasing core diameter enhances the bandwidth. As a result, a large core diameter combined with a reasonable outside diameter is desirable. But, in changing a fiber geometrical dimensions, one must consider the tradeoff relation between increased bandwidth and loss. This aspect is worth being investigated in further work.

Because the present dispersion model has the merit of incorporating all the main mechanisms involved, it offers the possibility of accurately predicting the information-carrying capacity of GRIN fibers, provided that correct parameter values are used. For the moment, owing to the difficulty of practically realizing the full and uniform launching condition, the experiment has not been done yet, but is planned for the future. Further extensions

of this work equally seem desirable: The introduction of the distributed loss and mode-coupling will cause both the optimum index exponent and the bandwidth-distance product to become length dependent. One foreseeable consequence of this is that the traditional characterization of MMF dispersion by a constant bandwidth-distance product will no longer be meaningful. Instead, the accurate determination of the bandwidth against length characteristic is actually of interest for the manufacturers and users of fiber-optic systems. In this way, on can deduce sample lengths over which gigabit Ethernet could comfortably be implemented. This is the first aspect being investigated with the aid of the present full theory. The second aspect is relative to the effect of different launching of the fiber. The present analysis was carried out under the assumption that a large number of modes are excited at the fiber input. A variety of launching techniques have been recently suggested in view of overcoming the intermodal dispersion [8], [9]. It can be easily imagined that for such alternatives based on restricted launching, the bandwidth advantage that can be obtained from the coupling of a large number of modes may no longer be true. Under restricted launch condition, indeed, mode-coupling may significantly limit the baseband bandwidth depending on the transmission length. As a matter of fact, even if a few low-order modes are initially excited, the power will gradually tend to spill out into higher order modes as light propagates down the fiber, thereby reducing the modal bandwidth at more or less long term. This trend should be resisted by the speed averaging effect of the coupling, but only the quantitative study will allow for drawing clear conclusions. Moreover, since both the restricted launching and the traditional use of fiber provide a bandwidth enhancement, it would be of interest to comparatively analyze these methods in order to provide guidelines for the best choice of technique for various LAN and interconnect systems.

ACKNOWLEDGMENT

The author would like to acknowledge the continuous and helpful discussions with Prof. G. D. Khoe, Dr. H. de Waardt, and Ir. H. P. A. van den Boom. He would equally like to thank Plasma Optical Fiber for making the fibers and for supplying his research group with samples. He would also like to acknowledge useful discussions with Dr. T. Breuls, Ir. G. Kuyt and Ir. M. de Fouw (from Plasma Optical Fiber) during the course of this study. He would also wish to thank the anonymous reviewers for their indepth comments on the manuscript.

REFERENCES

[1] R. E. Epworth, "The phenomenon of modal noise in analog and digital optical fiber systems," in *Proc. 4th ECOC*, Genova, Italy, 1978, pp. 492–501.

[2] R. J. S. Bates, D. M. Kuchta, and K. P. Jackson, "Improved multimode fiber link BER calculations due to modal noise and non self-pulsating laser diodes," *Optic. Quantum Electron.*, vol. 27, pp. 203–224, 1995.

[3] D. G. Cunningham, D. C. Hanson, M. C. Nowell, and C. S. Joiner, "Developing leading-edge fiber-optic network link standards," *The Hewlett-Packard J.*, pp. 62–73, Dec. 1997.

[4] *Information technology—Generic cabling for consumer premises*, ISO/IEC 11801: 1995 (E).

[5] *Mode scrambler requirements for overfilled launching conditions to multimode fibers*, EIA/TIA 455-54A.

[6] R. Olshansky and D. B. Keck, "Pulse broadening in graded-index optical fibers," *Appl. Opt.*, vol. 15, pp. 483–491, 1976.

[7] M. J. Adams, D. N. Payne, F. M. E. Sladen, and A. H. Hartog, "Optimum operating wavelength for chromatic equalization in multimode optical fibers," *Electron. Lett.*, vol. 14, pp. 64–66, 1978.

[8] Z. Haas and M. A. Santoro, "A mode-filtering scheme for improvement of the bandwidth-distance product in multimode fiber systems," *J. Lightwave Technol.*, vol. 11, pp. 1125–1131, 1993.

[9] L. Raddatz, I. H. White, D. G. Cunningham, and M. C. Nowell, "An experimental and theoretical study of the offset launch technique for the enhancement of the bandwidth of multimode fiber links," *J. Lightwave Technol.*, vol. 16, pp. 324–331, 1998.

[10] M. J. Yadlowsky and A. R. Mickelson, "Distributed loss and their effects on time-dependent propagation in multimode fibers," *Appl. Opt.*, vol. 32, pp. 6664–6678, 1993.

[11] D. Gloge, "Impulse response of clad optical multimode fibers," *Bell Syst. Tech. J.*, vol. 52, pp. 801–817, 1973.

[12] R. Olshansky, "Mode coupling effects in graded-index optical fibers," *Appl. Opt.*, vol. 14, pp. 935–945, 1975.

[13] ——, "Multiple-α index profiles," *Appl. Opt.*, vol. 18, pp. 683–689, 1979.

[14] A. R. Mickelson and M. Eriksrud, "Mode-continuum approximation in optical fibers," *Opt. Lett.*, vol. 7, pp. 573–574, 1982.

[15] G. J. Meslener, "Chromatic induced distortion of modulated monochromatic light employing direct modulation," *IEEE J. Quantum Electron.*, vol. QE-20, pp. 1208–1216, 1984.

[16] S. E. Miller and A. G. Chenoweth, Eds., *Optcal Fiber Telecommunications*. New York: Academic, 1979.

[17] S. D. Personick, "Baseband linearity and equalization in fiber optic digital communication systems," *Bell Syst. Tech. J.*, vol. 52, pp. 1175–1195, 1973.

[18] D. G. Duff, "Computer-aided design of digital lightwave systems," *IEEE J. Select. Areas Commun.*, vol. SAC-2, pp. 171–185, 1984.

[19] J. Gimlett and N. Cheung, "Dispersion penalty analysis for LED/single-mode fiber transmission systems," *J. Lightwave Technol.*, vol. LT-4, pp. 1381–1392, 1986.

[20] T. P. Lee, C. A. Burrus, D. Marcuse, A. G. Dentai, and R. J. Nelson, "Measurement of beam parameters of index-guided and gain-guided single-frequency InGaAsP injection lasers," *Electron. Lett.*, vol. 18, pp. 902–904, 1982.

[21] E.-G. Neumann, *Single-Mode Fibers*. Berlin, Germany: Springer-Verlag, 1988, pp. 246–247.

[22] D. Gloge, "Optical power flow in multimode fibers," *Bell Syst. Tech. J.*, vol. 51, pp. 1767–1783, 1972.

[23] R. Olshansky and D. A. Nolan, "Mode-dependent attenuation of optical fibers: Excess loss," *Appl. Opt.*, vol. 15, pp. 1045–1047, 1976.

[24] D. Gloge, "Weakly guiding fibers," *Appl. Opt.*, vol. 10, pp. 2252–2258, 1971.

[25] D. Marcuse, "Coupled mode theory of round optical fibers," *Bell Syst. Tech. J.*, vol. 52, pp. 817–843, 1973.

[26] J. N. Kutz, J. A. Cox, and D. Smith, "Mode mixing and power diffusion in multimode optical fibers," *J. Lightwave Technol.*, vol. 16, pp. 1195–1202, 1998.

[27] R. Olshansky, "Distortion losses in cabled optical fibers," *Appl. Opt.*, vol. 14, pp. 20–21, 1975.

[28] K. Nagano and S. Kawakami, "Measurement of mode conversion coefficients in graded-index fibers," *Appl. Opt.*, vol. 19, pp. 2426–2434, 1980.

[29] W. B. Gardner, "Microbending loss in optical fibers," *Bell Syst. Tech. J.*, vol. 54, pp. 457–465, 1975.

[30] M. Rousseau and L. Jeunhomme, "Numerical solution of the coupled-power equation in step-index optical fibers," *IEEE Trans. Microwave Theory Tech.*, vol. MTT-25, pp. 577–585, 1977.

[31] ——, "Optimum index profile in multimode optical fiber with respect to mode coupling," *Opt. Commun.*, vol. 23, pp. 275–278, 1977.

[32] T. P. Tanaka and S. Yamada, "Numerical solution of power flow in multimode W-type optical fibers," *Appl. Opt.*, vol. 19, pp. 1647–1652, 1980.

[33] W. Hermann and D. U. Wiechert, "Refractive index measurement on PCVD-bulk material," Philips Research Laboratories, Aachen, Germany, Internal Rep., 1988.

[34] S. D. Personick, "Time dispersion in dielectric waveguides," *Bell Syst. Tech. J.*, vol. 50, pp. 843–859, 1971.

[35] R. van Laere, S. Alers, and G. Kuyt, "Metingen aan vezels uit een voorvorm met een bewuste dip," Plasma Optical Fiber BV, Eindhoven, The Netherlands, Intern. Rep. TM97/171, 1997.

[36] M. K. Soudagar and A. A. Wali, "Pulse broadening in graded-index optical fibers: Errata," *Appl. Opt.*, vol. 32, p. 6678, 1993.

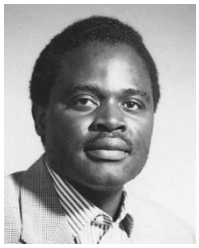

G. Yabre (M'97) was born in Boutaya-P/Zabré, Burkina Faso, in 1962. He received the DEA degree in electronics and the doctorate degree in optronics, both from the University of Brest, France, in 1989 and 1993, respectively.

From 1989 to 1995, he worked in the RESO Laboratory at the "Ecole Nationale d'Ingénieurs de Brest," France. He is now with COBRA, Interuniversity Research Institute, Eindhoven University of Technology, The Netherlands. During his previous post, his research activities were focused on semiconductor laser nonlinearities, linearization alternatives, injection-locking, subcarrier-multiplexing techniques, broad-band optical communication systems, and networks. He is currently working mostly on communication multimode optical fibers and related systems.

Dr. Yabre has served as a reviewer for the IEEE/OSA JOURNAL OF LIGHTWAVE TECHNOLOGY, IEEE TRANSACTIONS ON MICROWAVE THEORY AND TECHNIQUES, and *Optics Communications.*